 CMES, vol.102, no.1, pp.83-102, 2014

# A Level-set Algorithm for Simulating Wildfire Spread

**T. Ghisu**[1], **B. Arca**[2], **G. Pellizzaro**[2] and **P. Duce**[2]

**Abstract:** Level-set approaches are efficient and versatile methods for solving interface tracking problems and have been used in recent years to describe wildland fire propagation. Being based on an Eulerian description of the spread problem, their numerical implementation offers improved computational agility and better portability to parallel computing environments with respect to vector-based simulators. The use of a continuous representation of the fire perimeter in place of the binary formulation used in Cellular Automata avoids the commonly observed distortion of the fire shape. This work presents an algorithm for fire-spread simulation based on a level-set formulation. The results are compared to the ones obtained by two well-known Cellular Automata simulators under homogeneous conditions, and to the ones given by a well-know vector-based fire-spread simulator under realistic slope and wind conditions. According to this work, the level-set approach provides better results, in terms of accuracy, at a much reduced computational cost.

**Keywords:** Wildfire spread, level-set, cellular automata, Huygens principle.

## 1 Introduction

Methods for simulating wildland fires range from purely physical models (those based on the analysis of the physics and chemistry involved in the combustion of biomass fuel and its interaction with the atmosphere) to purely empirical models (those based on a statistical regression of the observed fire behavior) [Sullivan (2009a)]. As a full formulation of the equations governing a wildland fire is still not computationally feasible, a number of simplifications are often used in physical models: simplified chemistry, averaging (time-averaging or low-pass filtering), turbulence modeling, etc. Even with these assumptions, physical and quasi-physical models are in most cases several orders of magnitude slower than real-time, even on relatively large supercomputers, thus limiting their use for operational purposes (in 2007, a high-intensity fire simulation with 16 million grid cells within a $1.5 \times 1.5$

[1] Dipartment of Mechanical, Chemical and Materials Engineering, University of Cagliari, Italy
[2] Institute of Biometeorology, National Research Council, Italy

km domain took 0.44 processing hours for every second of simulated time [Mell, Jenkins, Gould, and Cheney (2007)] and, even if the current 30% yearly increase in computational power is maintained [Byrne, Oliner, and Sichel (2013)], it would take several decades before a similar model can be used for real-time applications at a comprensorial level). On the contrary, empirical and semi-empirical models, being based on a regression of experimental data, can provide faster-than-real-time predictions to fire spread problems (reliable when caution is placed on their limits of applicability [Perry (1998)]) and have become the basis of operational fire behavior models in use today [Sullivan (2009b)].

Empirical (and quasi-empirical) simulators are based on the combination of two elements: a fire-behavior model and a fire-spread method. *Fire-behavior models* estimate fire-behavior and spread characteristics that are important for fire suppression planning (such as rate of spread and fireline intensity) as a function of a number of independent variables (wind speed, terrain slope, fuel moisture, fuel load, fuel density, etc.). One of the most renowned is the model of Rothermel [Rothermel (1972, 1983)], which was developed based on a large number of laboratory experiments on surface fires of varying characteristics and forms the foundation of many fire-spread simulators in the United States and in Mediterranean Europe [Finney (2004); Lopes, Cruz, and Viegas (2002); Peterson, Morais, Calson, Dennison, Roberts, Moritz, and Weise (2009)]. Similar models have been developed in Australia [McArthur (1966)], Canada [Van Wagner (1998)] and other parts of the world. *Fire-spread methods* define the rules for evolving the fire perimeter across a landscape, based on the local characteristic of fuel, weather and topography.

Existing fire-spread techniques can be split into two categories. The first category goes under the name of *vector implementation* and treats the fire perimeter as a closed curve, discretized through a number of points, each one expanding based on the given spread model and the local conditions (fuel, weather and topography). The outer shape formed by all individual fires constitutes the new perimeter, which is further discretized and expanded. This approach was first introduced as the Huygens' principle for fire-spread simulation by [Anderson, Catchpole, De Mestre, and Parkes (1982)], using an ellipse to define the local shape of new fires. The second category – *raster implementation* – treats the problem by mean of a group of contiguous cells that can be either inactive (burnt or not burning) or active. A set of rules defines the spread mechanism from a cell to its neighbors, usually based on time-of-arrival or heat-accumulation approaches [Peterson, Morais, Calson, Dennison, Roberts, Moritz, and Weise (2009)].

Under homogeneous conditions (i.e. constant fuels, weather and topography), wildland fires have been observed to produce regular shapes, such as ellipses, double ellipses and ovoids. Richards [Richards (1995)] provides a mathematical formulation for the spread rate as a function of the angle from the direction of maximum spread for several of the observed shapes. Green *et al.* [Green, Gill, and Noble (1983)] compare experimental burned areas under homogeneous conditions, concluding that a simple ellipse could fit fire growth data as well as other shapes. The elliptic fire-spread template of Anderson *et al.* [Anderson, Catchpole, De Mestre, and Parkes (1982)] is used in FARSITE [Finney (2004)] and many other fire-spread simulators. In real conditions, wildland fires produce shapes different from the regular shapes mentioned above and require some form of spatial and temporal discretization to account for landscape and weather non-homogeneity.

The main weakness of vector-based approaches is the need for a computationally expensive algorithm for generating the convex hull fire-spread perimeter at each time step, especially in the presence of fire crossovers and unburned islands [Glasa and Halada (2008)]. Approaches based on raster implementations tend to be computationally more efficient, but can suffer from significant distortion of the produced fire shape: under constant wind and homogeneous landscape conditions, the heading portion of the fire perimeter tends to be angular rather than rounded [Karafyllidis and Thanailakis (1997)] due to the constraints of the grid cell restriction to eight directions of movement [Ball and Guertin (1992)]. These inaccuracies lead to modified predictions even in real landscape situations [Peterson, Morais, Calson, Dennison, Roberts, Moritz, and Weise (2009)].

A number of authors make use of larger neighborhoods, thus increasing the number of fire spread directions allowed [French, Anderson, and Catchpole (1990)] and mitigating the distortion of the theoretically elliptic shape. The same result can also be achieved by mean of a Minimum Travel Time (MTT) algorithm: the work of Finney [Finney (2002)] demonstrates how the use of an indefinitely large neighborhood leads to results equivalent to the ones given by a vector implementation, at the cost of larger computational costs and, more importantly, of large errors in the presence of real landscapes characterized by fuel and weather variability [Peterson, Morais, Calson, Dennison, Roberts, Moritz, and Weise (2009)]. Alternative discretizations have been also used: Frandsen and Andrews [Frandsen and Andrews (1979)] and Hernández-Encinas *et al.* [Hernández Encinas, Hoya White, Martín del Rey, and Rodríguez Sánchez (2007)] employed hexagonal cells suffering from the same distortion problems found in the square model, Johnston *et al.* [Johnston, Kelso, and Milne (2008)] employed an irregular grid to avoid directional biasing in fire-front propagation. To improve the produced fire perimeter, they modified the rate of spread function with the inclusion of two terms: the first one divides a region where the backing rate of spread is employed from one where a variable rate of spread is used, the latter increases the maximum rate of spread to allow for the fact that on an irregular grid fire cannot travel in a straight line, but follows an irregular path dictated by the cells' connections. The first factor is chosen from experience, while for the second factor the authors use a parametric search aimed at matching the rate of spread in the direction of maximum propagation. The results for the maximum rate of spread are promising, but little insight is given on the mitigation of the elliptic shape distortion. Trunfio *et al.* [Trunfio, D'Ambrosio, Rongo, Spataro, and Di Gregorio (2011)] suggest an improved algorithm for simulating wildfire spread through Cellular Automata, which, not restricting the ignition points' locations to the cell centers, does not limit the fire spread to the eight directions (or more if larger neighborhoods are used) defined by the raster discretization, producing shapes more closely resembling the theoretically elliptic shape. This is achieved at the price of an increased computational cost, due to the calculation of the position of the new ignition point within each raster cell, making the solution approach a hybrid between a Cellular Automata and a vector implementation.

In recent years, an alternative approach has gained attention: the level-set methodology is a versatile technique for general front tracking problems. It was first developed by Osher and Sethian [Osher and Sethian (1988)] to express the motion of $N-1$ dimensional surfaces in $N$ spatial dimensions. The method makes use of a Hamilton-Jacobi equation (a hyperbolic partial differential equation) to describe the propagation of the fire front, which is defined implicitly by mean of a level-set function. The differential equation can be solved using an appropriate numerical method for hyperbolic conservation laws and does not require the addition of new computational elements (unlike the vector implementation) as the simulation progresses, being able to deal with complex topological features (merging of fire fronts or formation of islands) without any additional requirements. This approach has been employed with success in several areas: solution of complex multi-phase flows [Balabel (2012, 2013); Wang, Li, Yang, and Hill (2013)], topology optimization [Matsumoto, Yamada, Takahashi, Zheng, and Harada (2011); Li, Ouyang, Wu, and Xu (2011)], injection moliding simulation [Yang, Ouyang, Jiang, and Liu (2010); Li, Ouyang, Wu, and Xu (2011)], passive transport problems [Mai-Cao and Tran-Cong (2008)].

Recently, Mallet *et al.* [Mallet, Keyes, and Fendell (2009)] made use of a level-set method combined with a simple expression for the advection velocity, defined as a trigonometric combination of three values for flank, head and rear fire-spread rates. Rehm *et al.* [Rehm and Mcdermott (2010)] used the same approach to compare Lagrangian and Eulerian formulations of the fire-spread problem, noting their equivalence for simple scenarios. Mandel *et al.* [Mandel, Beezley, and Kochanski (2011)] coupled a level-set formulation for fire-front propagation with the Weather Research and Forecasting (WRF) Model, a mesoscale numerical weather prediction system used both for forecasting and atmospheric research purposes, allowing the two-way interaction between fire and atmosphere to be calculated and accounted for in fire-propagation simulations.

The common distortion problem found in Cellular Automata is due to the limitation of the spread to a number of fixed directions (eight in the presence of the simplest approach, where fire can only spread from one cell to its immediate neighbors), which in turn depends on the binary nature of Cellular Automata (each cell can be either in burning or non-burning) rather than on the raster discretization itself. Level-set methods do not limit the position of the fire-front to the nodes of the numerical grid and therefore can provide a much more precise description of the spread phenomenon.

Other advantages of the level-set approach are its computational agility and portability to parallel computing environments, while the increased computational cost (which for a one-dimensional interface moving in a two-dimensional space is $O(n^2)$ per time iteration, with $n$ number of points in each spatial dimension) can be reduced by mean of a narrow-band method ($O(kn)$, where $k$ is a constant depending on the width of the narrow-band tube) [Adalsteinsson and Sethian (1995)]. Despite these advantages, a validation for simple fire-propagation problems has not yet been presented.

This work presents a level-set approach to fire propagation that allows the simulated fire perimeters to approximate the expected elliptic fire shapes more closely than other raster-based techinques such as Cellular Automata. The results are compared to the ones obtained by other cell-based simulators based on a Cellular Automata paradigm [Peterson, Morais, Calson, Dennison, Roberts, Moritz, and Weise (2009); Trunfio, D'Ambrosio, Rongo, Spataro, and Di Gregorio (2011)] and show a significantly improved accuracy, in the presence of a much reduced computational cost.

The rest of this paper is organized as follows. Section 2 summarizes the semi-empirical equations of Rothermel [Rothermel (1972)] and Richards [Richards (1995)], used as the basis for this work. Section 3 provides a brief introduction to level-set methods. Section 4 analyzes the predicted fire perimeters, both for homogeneous and realistic spread conditions. Section 5 draws some conclusions and outlines future directions.

## 2 Fire-spread Model

The fire-spread model is based on Rothermel's surface fire spread model [Rothermel (1972)]. This choice was dictated by its application to many fuels around the world, such as logging slash, grasslands and shrublands and by its use in different software for fire behavior prediction such as FIREMAP [Ball and Guertin (1992)], FARSITE [Finney (2004)], FireStation [Lopes, Cruz, and Viegas (2002)], FlamMap [Finney (2006)], and HFIRE [Peterson, Morais, Calson, Dennison, Roberts, Moritz, and Weise (2009)].

A list of input parameters required by the fire propagation model is given in Table 1. The model's outputs are given in Table 2. Fuel properties are generally supplied separately for live and dead fuels, for different size classes. Properties are averaged between size classes using the surface-to-volume ratio as weighting factor, while live and dead fuels are treated separately. A full derivation and description of the parameters in use is given in [Rothermel (1972)].

Table 1: Input parameters required by Rothermel's model [Rothermel (1972)]

| Description | Symbol | Units |
|---|---|---|
| Fuel load | $W_0$ | kg m$^{-2}$ |
| Fuel depth | $\delta$ | m |
| Surface-to-volume ratio | $\sigma$ | m$^{-1}$ |
| Fuel heat content | $h$ | kJ kg$^{-1}$ |
| Fuel moisture content | $M_f$ | - |
| Fuel moisture content of extinction | $M_x$ | - |
| Ovendry particle density | $\rho_p$ | kg m$^{-1}$ |
| Fuel particle total mineral content | $S_T$ | - |
| Fuel particle effective mineral content | $S_e$ | - |
| Midflame-height wind speed | $U_m$ | m s$^{-1}$ |
| Terrain slope | $\phi$ | degrees |

$I_R$ and $R_0$ represent reaction intensity and rate of spread on a flat terrain with no wind. In the presence of wind and slope, these two parameters are multiplied by $(1+\phi_w+\phi_s)$, where $\phi_w$ and $\phi_s$ are two fire-intensification factors which depend on local wind and terrain slope. The direction of maximum spread is obtained through a vectorial summation of the dimensionless coefficients for wind speed and slope [Finney (2004)]. The two-dimensional fire-spread rule used is the one described in [Alexander (1985)], subsequently adapted by [Finney (2004)]. The ellipse length-to-width ratio can be calculated as:

$$LW = 0.936e^{50.5U_{eq}} + 0.461e^{-30.5U_{eq}} - 0.397 \tag{1}$$

where the equivalent wind speed $U_{eq}$ (in ms$^{-1}$) is the wind speed that alone would produce the combined effect of actual wind and terrain slope. Assuming the fire origin to be located at the rear focus of the ellipse, the fire-spread rate can be calculated as a function of the angle $\theta$, measured from the direction of maximum spread.

$$R(\theta) = R_0 \frac{1-\overline{E}}{1-\overline{E}cos(\theta)} \tag{2}$$

Table 2: Outputs from Rothermel's model [Rothermel (1972)]

| Description | Symbol | Units | Equation |
|---|---|---|---|
| | $A$ | - | $A = \frac{1}{4.239\sigma^{0.1}-7.27}$ |
| | $B$ | - | $B = 0.0133\sigma^{0.54}$ |
| | $C$ | - | $C = 7.47exp(-0.0693\sigma^{0.55})$ |
| | $E$ | - | $E = 0.715exp(-1.079 \times 10^{-4}\sigma)$ |
| Maximum reaction velocity | $\Gamma'_{max}$ | $s^{-1}$ | $\Gamma'_{max} = \frac{\sigma^{1.5}}{1171.27+3.564\sigma^{1.5})}$ |
| Optimum reaction velocity | $\Gamma'$ | $s^{-1}$ | $\Gamma' = \Gamma'_{max}(\frac{\beta}{\beta_{op}})^A exp([A(1-\frac{\beta}{\beta_{op}})])$ |
| Optimum packing ratio | $\beta_{op}$ | - | $\beta_{op} = 3.348\sigma^{-0.8189}$ |
| Moisture damping coefficient | $\eta_M$ | - | $\eta_M = 1 - 2.59\frac{M_f}{M_x} + 5.11(\frac{M_f}{M_x})^2 - 3.52(\frac{M_f}{M_x})^3$ |
| Mineral damping coefficient | $\eta_S$ | - | $\eta_M = 0.174S_e^{-0.19}$ |
| Propagating flux ratio | $\xi$ | - | $\xi = \frac{exp[(0.792+0.376\sigma^{0.5})(\beta+0.1)}{192+0.0791\sigma}$ |
| Net fuel loading | $W_n$ | kg $m^{-2}$ | $W_n = \frac{W_0}{1+S_T}$ |
| Ovendry bulk density $\rho_b$ | kg $m^{-3}$ | | $\rho_b = \frac{W_0}{\delta}$ |
| Effective heating number | $\varepsilon$ | - | $\varepsilon = exp(-4527.56\sigma^{-1})$ |
| Heat of preignition | $Q_{ig}$ | kJ $kg^{-1}$ | $Q_{ig} = 522 + 2332M_f$ |
| Packing ratio | $\beta$ | - | $\beta = \frac{\rho_b}{\rho_p}$ |
| **Reaction intensity** | $I_R$ | kJ $m^2$ s−1 | $I_R = \Gamma' W_n h \eta_M \eta_S$ |
| **Rate of spread** | $R_0$ | m $s^{-1}$ | $R_0 = \frac{I_R\xi}{\rho_b \varepsilon Q_{ig}}$ |
| **Wind factor** | $\phi_w$ | - | $\phi_w = CU^B(\frac{\beta}{\beta_o p})^{-E}$ |
| **Slope factor** | $\phi_s$ | - | $\phi_s = 5.275\beta^{-0.3}(tan\phi)^2$ |

where $\overline{E}$ is the ellipse eccentricity, defined as $\sqrt{1-1/LW^2}$. Alternatively, the same can be calculated as a function of the angle $\theta'$ between the normal to the fire surface and the direction of maximum spread:

$$R(\theta') = (acos(\theta'))^2 + (bsin(\theta'))^2 + ccos(\theta') \tag{3}$$

where $a$, $b$ and $c$ are respectively the ellipse's semi-major and semi-minor axes and semi-focal-length.

## 3 Fire-front Propagation using a Level-set Approach

Level-set methods are Eulerian schemes for tracking fronts that propagate with a given speed function (which can depend on position, time and other local properties such as normal direction and local curvature [Osher and Sethian (1988)]). The basic idea is to use an implicit definition of the front $\Gamma$ by mean of a function $\psi : \mathbb{R}^N \times [0, T_f] \to \mathbb{R}$ such that

$$\forall t \in [0, T_f] \qquad \Gamma(t) = \left\{ \mathbf{x} \in \mathbb{R}^N | \psi(\mathbf{x}, t) = 0 \right\} \tag{4}$$

The partial differential equation defining the evolution of the front can be obtained by differentiating the equation for the fire front with respect to time:

$$\frac{\partial \psi}{\partial t} + \mathbf{R} \cdot \nabla \psi = \mathbf{0} \tag{5}$$

where $\mathbf{R}$ is the front propagation speed. To simplify the solution of equation (5), the spread rate can be calculated as a a function of the angle between the normal to the level-set function and the maximum-spread direction. In this case, the front propagation speed $\mathbf{R}$ will be calculated from equation (3) and parallel to $\nabla \psi$.

On Cartesian grids, equation (5) can be solved using a Finite Difference approach. To preserve stability, special care needs to be placed in the approximation of spatial derivatives. The simplest stable scheme is a first-order upwind. For the x-derivative it reads:

$$\frac{\partial \psi}{\partial x} = \begin{cases} \frac{\psi_{i,j} - \psi_{i-1,j}}{\Delta x} & \text{if } R_x \geq 0 \\ \frac{\psi_{i+1,j} - \psi_{i,j}}{\Delta x} & \text{otherwise} \end{cases} \tag{6}$$

where $R_x$ is the x-component or $\mathbf{R}$. Similarly, the time derivative in equation (5) can be approximated with a first-order explicit scheme (Euler's method):

$$\frac{\partial \psi}{\partial t} = \frac{\psi_{i,j}^{n+1} - \psi_{i,j}^{n}}{\Delta t} \tag{7}$$

where the superscripts represent the time step. This approach is first-order accurate in both time and space: higher-order discretizations can be used, but are not considered in this study due to the uncertainties in the estimation of the fire propagation rate. For an explicit scheme, the maximum stable time step is related to the grid spacing by the Courant-Friedrichs-Lewy (CFL) condition:

$$\max \left( \frac{R \Delta t}{\Delta x} \right) \leq 1 \tag{8}$$

Neumann boundary conditions are used at the boundaries of the physical domain (i.e.$\frac{\partial \psi}{\partial x} = \frac{\partial \psi}{\partial y} = 0$). To approximate the fire front at time $t = 0$, the initial value of the level-set function can be chosen as the signed distance from the fireline [Mallet, Keyes, and Fendell (2009)]:

$$\psi(\mathbf{x}, t) = \begin{cases} \quad d_{\Gamma(t)}(\mathbf{x}) & \text{if } \mathbf{x} \text{ lies outside the front } \Gamma(\mathbf{x}) \\ - \quad d_{\Gamma(t)}(\mathbf{x}) & \text{if } \mathbf{x} \text{ lies inside the front } \Gamma(\mathbf{x}) \end{cases} \tag{9}$$

Alternatively, the level-set function can be initialized with a positive value in non-burnt regions and with a negative value in burnt regions.

### 3.1 Sloping Terrain

The equations introduced in Section 2 provide the rate of spread relative to the ground surface. Therefore, in the presence of sloping terrain, the value needs to be corrected to represent the rate of spread in the horizontal coordinate system.

$$R_x = R'_x cos(\delta_x) \quad (10)$$

$$R_y = R'_y cos(\delta_y) \quad (11)$$

where $R'_x$ and $R'_y$ are the rate of spread components in a coordinate system parallel to the ground, $R_x$ and $R_y$ are the rate of spread components in a horizontal coordinate system and $\delta_x$ and $\delta_y$ the slope components.

### 3.2 Model Evaluation

To evaluate the performance of the level-set algorithm, the following metrics were adopted:

$$\lambda_u = \frac{|R-S|}{|R|} \quad (12)$$

$$\lambda_o = \frac{|S-R|}{|S|} \quad (13)$$

$$\lambda_s = \frac{|R \cup S| - |R \cap S|}{|R \cup S|} \quad (14)$$

where $R$ represents the set of cells defining the expected fire shape, $S$ the set of cells defining the simulated fire shape and the operator $|.|$ gives the size of a set. Consequently, $\lambda_u$ and $\lambda_o$ represent the underpredicted and overpredicted fire area ratios, respectively, while $\lambda_s$ is a measure of the level of disagreement between the two predictions. To compute the set of cells defining the expected fire shape, a cell was considered burnt when its center fell inside the fire ellipse. To compute the predicted fire shape, a cell was considered burnt when the corresponding value for the level-set function was less than zero.

The same metrics were adopted by [Trunfio, D'Ambrosio, Rongo, Spataro, and Di Gregorio (2011)] to evaluate the performance of their proposed Cellular Automata approach in comparison to the one of [Peterson, Morais, Calson, Dennison, Roberts, Moritz, and Weise (2009)].

# 4 Results

## *4.1 Homogeneous Fire-spread Conditions*

The fire shapes obtained with the level-set approach for different values of ellipse eccentricity (0.5, 0.7, 0.9 and 0.95) are shown in Figures 1, 2, 3 and 4, respectively, for different wind angles. The corresponding values for error factors $\lambda_s$, $\lambda_u$ and $\lambda_o$ are summarized in Table 3, where they are compared to the ones obtained through to two well-known Cellular Automata (raster-based) simulators – the one proposed by [Peterson, Morais, Calson, Dennison, Roberts, Moritz, and Weise (2009)] (labeled RCA) and the one proposed by [Trunfio, D'Ambrosio, Rongo, Spataro, and Di Gregorio (2011)] (ECA) – using both a 8-cell and a 24-cell neighborhood. The benefits of the level-set approach are evident, both graphically (through the similarity between expected and predicted fire shapes) and numerically. Considering the largest eccentricity case with wind in the direction of one of the grid axes, the reduction in shape factor's value is 93.9% relative to the 24-cell neighborhood RCA and 70.8% relative to the 24-cell neighborhood ECA taken as reference. The error is equally divided between under- and over-predicted areas. Relatively to the reference algorithms, the under-prediction factor $\lambda_u$ is reduced by 97.1% (RCA) and 80% (ECA). The over-prediction factor $\lambda_o$ has also been reduced (-56%) relative to the one found in the 24-cell neighborhood ECA (the RCA has a zero value for $\lambda_o$). The influence of the effective wind direction on the fire shape is also minimal.

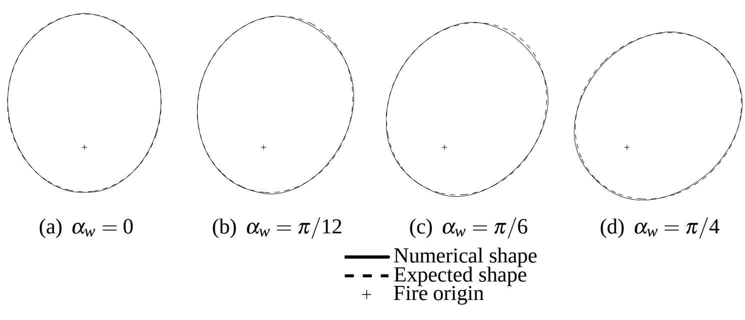


Figure 1: Comparison of expected and numerical two-dimensional fire-spread shapes under homogeneous conditions, for different wind angles ($\overline{E} = 0.50$)

Even if a comparison of the computational times required by different numerical algorithms is not straight-forward (they are highly dependent on the specific implementations), the potential for low running time of cell-based approaches is widely recognized, thanks to the avoidance of the de-looping algorithm necessary

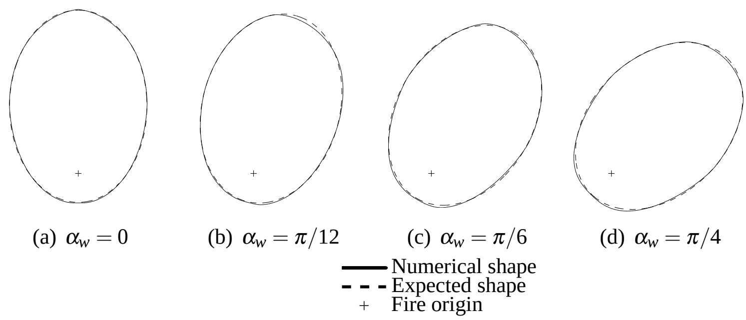


Figure 2: Comparison of expected and numerical two-dimensional fire-spread shapes under homogeneous conditions, for different wind angles ($\overline{E} = 0.70$)

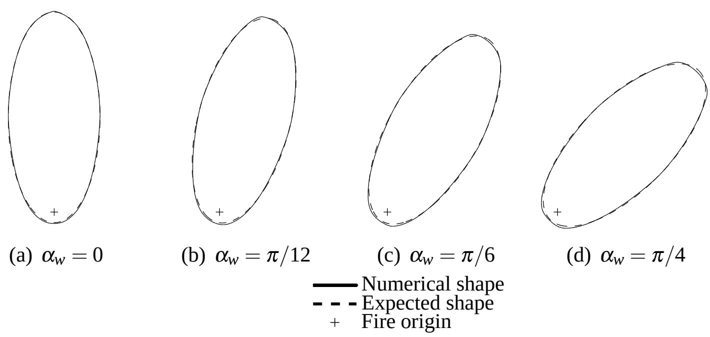


Figure 3: Comparison of expected and numerical two-dimensional fire-spread shapes under homogeneous conditions, for different wind angles ($\overline{E} = 0.90$)

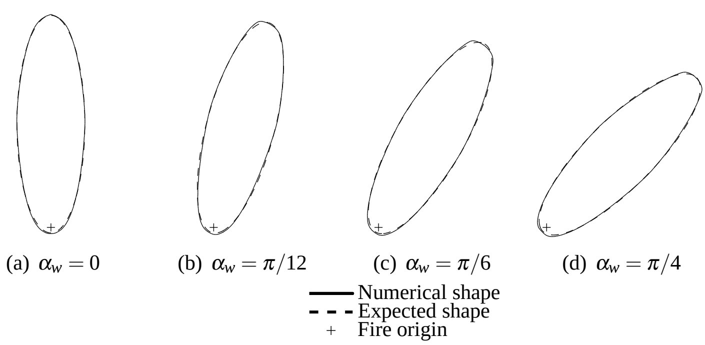


Figure 4: Comparison of expected and numerical two-dimensional fire-spread shapes under homogeneous conditions, for different wind angles ($\overline{E} = 0.95$)

Table 3: Dependence of Error Factors $\lambda_s$, $\lambda_u$ and $\lambda_o$ on the Wind Angle $\alpha_w$ (part 1)

| $\overline{E}$ | 0.50 | | | | 0.70 | | | |
|---|---|---|---|---|---|---|---|---|
| $\alpha_w$ | 0 | $\pi/12$ | $pi/6$ | $\pi/4$ | 0 | $\pi/12$ | $pi/6$ | $\pi/4$ |
| $\lambda_s$ | 0.010 | 0.014 | 0.019 | 0.019 | 0.014 | 0.020 | 0.021 | 0.020 |
| $\lambda_u$ | 0.005 | 0.007 | 0.010 | 0.010 | 0.007 | 0.010 | 0.011 | 0.010 |
| $\lambda_o$ | 0.005 | 0.007 | 0.010 | 0.010 | 0.007 | 0.010 | 0.010 | 0.010 |

Table 4: Dependence of Error Factors $\lambda_s$, $\lambda_u$ and $\lambda_o$ on the Wind Angle $\alpha_w$ (part 2)

| $\overline{E}$ | 0.90 | | | | 0.95 | | | |
|---|---|---|---|---|---|---|---|---|
| $\alpha_w$ | 0 | $\pi/12$ | $pi/6$ | $\pi/4$ | 0 | $\pi/12$ | $pi/6$ | $\pi/4$ |
| $\lambda_s$ | 0.016 | 0.022 | 0.023 | 0.023 | 0.021 | 0.027 | 0.024 | 0.025 |
| $\lambda_u$ | 0.008 | 0.011 | 0.011 | 0.011 | 0.010 | 0.014 | 0.012 | 0.013 |
| $\lambda_o$ | 0.008 | 0.011 | 0.012 | 0.012 | 0.011 | 0.014 | 0.012 | 0.012 |

to reconstruct the fire perimeter at the end of each time step in vector-based implementations. Other advantages of raster-based algorithms in general (and level-set approaches in particular) are their computational agility and portability to parallel computing environment. The governing partial differential equation does not need to be solved in every cell of the computational domain (this would make the algorithm O($n^2$), with $n$ number of computational points for each spatial dimension): the computational cost can be sensibly reduced by mean of a narrow-band approach, where only the cells lying within a certain distance from the fire-front are updated at each time step.

### *4.2 Comparison with FARSITE on Real Topographies*

In order to verify its performance on a realistic fire-spread problem, the level-set algorithm was compared to FARSITE [Finney (2004)] on a real topography under different wind conditions. FARSITE has been chosen as the reference simulator because the vector-based approach is the only one that produces perfectly elliptical fire-propagation fronts in homogeneous conditions and, for this reason, has been already taken as the reference by a number of different fire spread-simulators [Trunfio, D'Ambrosio, Rongo, Spataro, and Di Gregorio (2011); Finney (2006); Peterson, Morais, Calson, Dennison, Roberts, Moritz, and Weise (2009)], which report deviations in fire-perimeters and computational times relative to FARSITE.

Only surface fires have been considered, and spotting and acceleration modules were disabled in FARSITE, as the purpose of this exercise was to evaluate the performance of the fire-spread approach. The numerical grid used by the level-set solver is constituted by 1.44 million square cells with 10 meter sides. FARSITE does not make use of a fixed numerical grid, but discretizes the fire perimeter directly. The maximum distance between adjacent computational points and their maximum displacement has been set to values similar to the ones used by the level-set solver. A uniform fuel bed corresponding to the standard fuel model 1 (grass) [Anderson, Catchpole, De Mestre, and Parkes (1982)] was used.

Three scenarios were simulated: a zero-wind situation, a scenario with a 4.5 $ms^{-1}$ domain-averaged wind and one with a 9 $ms^{-1}$ domain-averaged wind (measured at 6.096 meters agl), directed from West to East. The three scenarios are labeled T0, T10 and T20, for simplicity. Gridded wind vectors were obtained through a mass-consistent approach [Forthofer (2007)].

According to FARSITE, the surface fire burned a total of 5.96 $km^2$ in 12 hours in T0, 12.07 $km^2$ in 4 hours in T1 and 7.08 $km^2$ in 1 hour in T2. Figures 5, 6 and 7 show a comparison of the fire shapes predicted by FARSITE and the level-set solver. The agreement is evident.

Tables 5, 6 and 7 report the shape disagreement factors for the three experiments, at four intermediate times. The values are lower than the ones reported by state-of-the-art Cellular Automata simulators on comparable fire-spread scenarios [Trunfio, D'Ambrosio, Rongo, Spataro, and Di Gregorio (2011)]. Table 8 compares the wall clock times: for complex simulations (the combined presence of variable slope and wind), the reduction in wall clock time can be of the order of 90%, larger than the one claimed by Cellular Automata approaches [Trunfio, D'Ambrosio, Rongo, Spataro, and Di Gregorio (2011)] and without the need of employing large neighborhoods [Peterson, Morais, Calson, Dennison, Roberts, Moritz, and Weise (2009); Finney (2006)] which could result in less accurate predictions in the presence of heterogeneous weather or landscape conditions but that are essential to reduce or eliminate the well known distortion problem or complex corrections to the basic fire-spread algorithm that inhevitably increase computational time [Trunfio, D'Ambrosio, Rongo, Spataro, and Di Gregorio (2011)].

Computational times are calculated in the case of a serial implementation: cell-based methods offer a better scalability in parallel computing environments, with potentially even more significant time savings. The simulations have been completed using one core from a dual quad-core 2.53 GHz Intel Xeon processor.

Table 5: Error Factors $\lambda_s$, $\lambda_u$ and $\lambda_o$ for the T0 experiment

| Elapsed Time | $\lambda_s$ | $\lambda_u$ | $\lambda_o$ |
|---|---|---|---|
| 3 hrs | 0.063 | 0.029 | 0.035 |
| 6 hrs | 0.062 | 0.025 | 0.039 |
| 9 hrs | 0.029 | 0.018 | 0.011 |
| 12 hrs | 0.029 | 0.010 | 0.019 |

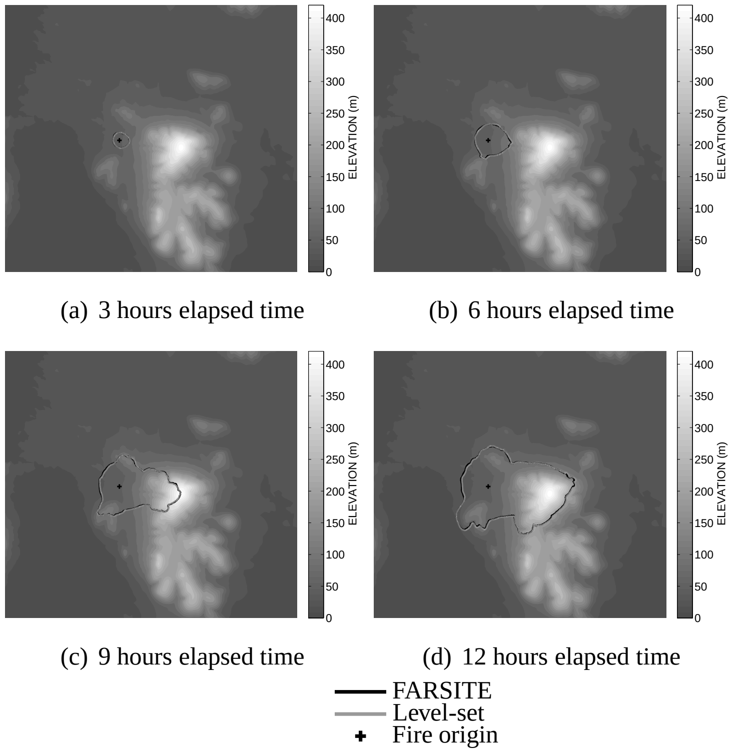


(a) 3 hours elapsed time (b) 6 hours elapsed time

(c) 9 hours elapsed time (d) 12 hours elapsed time

Figure 5: Comparison of fire perimeters predicted by FARSITE and the level-set solver (zero-wind conditions)

Table 6: Error Factors $\lambda_s$, $\lambda_u$ and $\lambda_o$ for the T1 experiment

| Elapsed Time | $\lambda_s$ | $\lambda_u$ | $\lambda_o$ |
|---|---|---|---|
| 1 hr | 0.046 | 0.010 | 0.036 |
| 2 hrs | 0.023 | 0.007 | 0.016 |
| 3 hrs | 0.019 | 0.008 | 0.014 |
| 4 hrs | 0.018 | 0.007 | 0.011 |

## 5 Conclusions

This work presents a level-set approach for wildland fire prediction. Level-set methods are Eulerian schemes for tracking fronts and present improved computational agility and better suitability to parallel environments relatively to Lagrangian approaches (vector-based simulators). With respect to other raster-based approaches

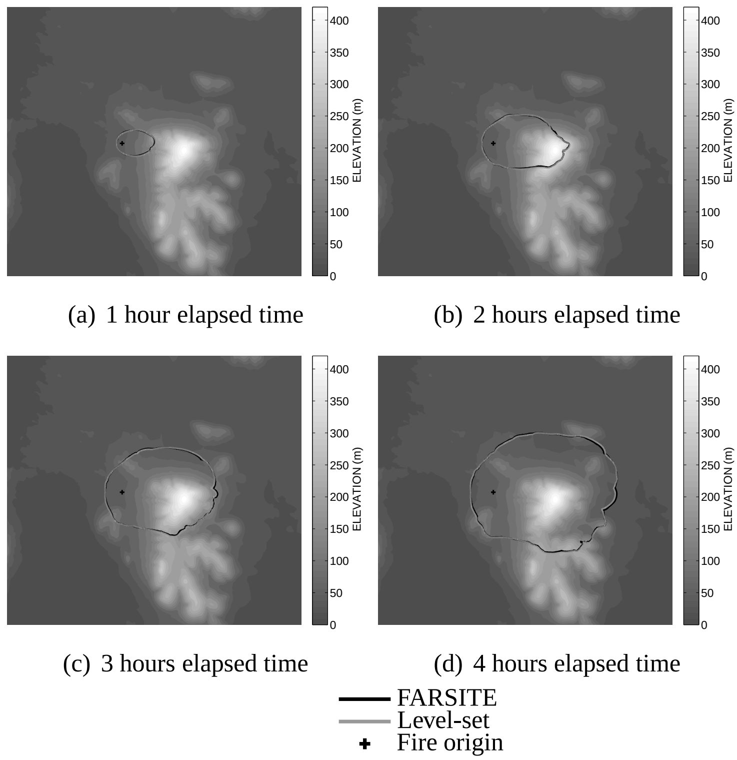


(a) 1 hour elapsed time (b) 2 hours elapsed time

(c) 3 hours elapsed time (d) 4 hours elapsed time

Figure 6: Comparison of fire perimeters predicted by FARSITE and the level-set solver (4.5 $ms^{-1}$ average wind conditions)

Table 7: Error Factors $\lambda_s$, $\lambda_u$ and $\lambda_o$ for the T2 experiment

| Elapsed Time | $\lambda_s$ | $\lambda_u$ | $\lambda_o$ |
|---|---|---|---|
| 15 mins | 0.047 | 0.007 | 0.040 |
| 30 mins | 0.044 | 0.021 | 0.024 |
| 45 mins | 0.031 | 0.016 | 0.015 |
| 1 hr | 0.026 | 0.008 | 0.018 |

Table 8: Comparison of Wall Clock Times between FARSITE and the level-set approach

| Experiment | FARSITE | Level-set |
|---|---|---|
| T0 | 979 s | 91 s |
| T1 | 738 s | 129 s |
| T2 | 382 s | 44 s |

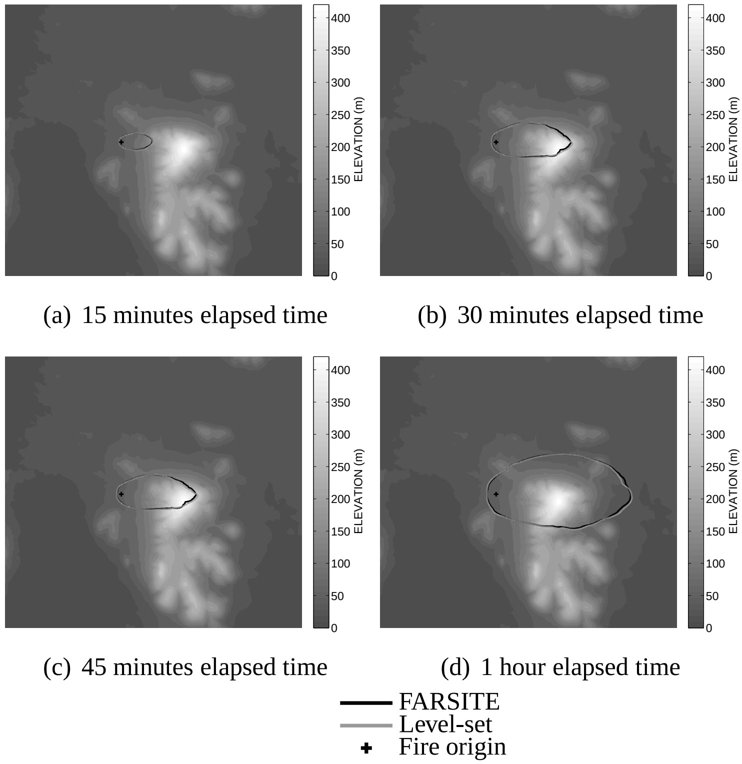


(a) 15 minutes elapsed time (b) 30 minutes elapsed time

(c) 45 minutes elapsed time (d) 1 hour elapsed time

Figure 7: Comparison of fire perimeters predicted by FARSITE and the level-set solver (9 $ms^{-1}$ average wind conditions)

(such as Cellular Automata), they do no suffer from the widely-documented distortion problem caused by the restriction of the spread-direction to (small) a number of fixed angles. The approach has been validated both under homogeneous conditions (with comparison to the theoretical fire shapes) and under realistic conditions (with comparison to the predictions from FARSITE [Finney (2004)], a well known vector-based fire-spread simulator). The values obtained for the error functions have been also compared to the results achieved by two well-known Cellular Automata [Peterson, Morais, Calson, Dennison, Roberts, Moritz, and Weise (2009); Trunfio, D'Ambrosio, Rongo, Spataro, and Di Gregorio (2011)]: the level-set approach achieves lower error factors in the presence of much reduced computational times.

The level-set method represents an efficient approach for fire-front propagation simulation. Future work includes further testing in real-world scenarios (including comparison to available experimental data), parallelization and implementation in Finite Volume formulation to simplify the connection to CFD solvers able to simulate the two-way interaction between fire and wind.

## References

**Adalsteinsson, D.; Sethian, J. A.** (1995): A fast Level Set Method for Propagating Interfaces. vol. 118, no. 2, pp. 269—-277.

**Alexander, M. E.** (1985): Estimating the length-to-breadth ratio of elliptical forest fire patterns. In *Proceedings of the 8th Conference on Fire and Forest Meteorology*, pp. 287—-304.

**Anderson, D. H.; Catchpole, E.; De Mestre, N. J.; Parkes, T.** (1982): Modeling the Spread of Grass Fires. *The Journal of the Australian Mathematical Society Series B Applied Mathematics*, vol. 23, no. 04, pp. 451–466.

**Balabel, A.** (2012): Numerical modelling of turbulence effects on droplet collision dynamics using the level set method. *CMES - Computer Modeling in Engineering and Sciences*, vol. 89, no. 4, pp. 283–301.

**Balabel, A.** (2013): Numerical modelling of liquid jet breakup by different liquid jet/air flow orientations using the level set method. *CMES - Computer Modeling in Engineering and Sciences*, vol. 95, no. 4, pp. 283–302.

**Ball, G. L. G.; Guertin, D. P.** (1992): Improved Fire Growth Modeling. *International Journal Of Wildland Fire*, vol. 2, no. 2, pp. 47–54.

**Byrne, D. M.; Oliner, S. D.; Sichel, D. E.** (2013): Is the information technology revolution over? *Finance and Economics Discussion Series*.

**Finney, M. A.** (2002): Fire growth using minimum travel time methods. *Sciences-New York*, pp. 1420–1424.

**Finney, M. A.** (2004): FARSITE: Fire area simulator-model development and evaluation. Technical Report RMRS-RP-4, USDA, Ogden, UT, 2004.

**Finney, M. A.** (2006): An overview of FlamMap fire modeleng capabilities. In *Fuels Management - How to Measure Success*, no. RMRS-P-41. USDA Forest Service.

**Forthofer, J. M.** (2007): *Modeling Wind in Complex Terrain for Use in Fire Spread Predictions*. PhD thesis, 2007.

**Frandsen, W. H.; Andrews, P. L.** (1979): Fire Behavior in Non-uniform Fuels. Technical report, USDA, Ogden, UT, 1979.

**French, I. A.; Anderson, D.; Catchpole, E. A.** (1990): Graphical Simulation of Bushfire Spread. *Mathematics and Computer Modelling*, vol. 13, no. 12, pp. 67–71.

**Glasa, J.; Halada, L.** (2008): On elliptical model for forest fire spread modeling and simulation. *Mathematics and Computers in Simulation*, vol. 78, no. 1, pp. 76–88.

**Green, D. G.; Gill, A. M.; Noble, I. R.** (1983): Fire shapes and the adequacy of fire-spread models. *Ecological Modelling*, vol. 20, no. 1, pp. 33–45.

**Hernández Encinas, L.; Hoya White, S.; Martín del Rey, A.; Rodríguez Sánchez, G.** (2007): Modelling forest fire spread using hexagonal cellular automata. *Applied Mathematical Modelling*, vol. 31, no. 6, pp. 1213–1227.

**Johnston, P.; Kelso, J.; Milne, G. J.** (2008): Efficient simulation of wildfire spread on an irregular grid. *International Journal of Wildland Fire*, vol. 17, no. 5, pp. 614—-627.

**Karafyllidis, I.; Thanailakis, A.** (1997): A model for predicting forest fire spreading using cellular automata. *Ecological Modelling*, vol. 99, no. 1, pp. 87–97.

**Li, Q.; Ouyang, J.; Wu, G.; Xu, X.** (2011): Numerical simulation of melt filling and gas penetration in gas assisted injection molding. *CMES - Computer Modeling in Engineering and Sciences*, vol. 82, no. 3-4, pp. 215–232.

**Lopes, A. M. G.; Cruz, M. G.; Viegas, D. X.** (2002): FireStation – an integrated software system for the numerical simulation of fire spread on complex topography. *Environmental Modelling Software*, vol. 17, no. 3, pp. 269–285.

**Mai-Cao, L.; Tran-Cong, T.** (2008): A meshless approach to capturing moving interfaces in passive transport problems. *CMES - Computer Modeling in Engineering and Sciences*, vol. 31, no. 3, pp. 157–188.

**Mallet, V.; Keyes, D.; Fendell, F.** (2009): Modeling wildland fire propagation with level set methods. *Computers & Mathematics with Applications*, vol. 57, no. 7, pp. 1089–1101.

**Mandel, J.; Beezley, J. D.; Kochanski, A. K.** (2011): Coupled atmosphere-wildland fire modeling with WRF-Fire version 3.3. *Geoscientific Model Development Discussions*, pp. 497–545.

**Matsumoto, T.; Yamada, T.; Takahashi, T.; Zheng, C.; Harada, S.** (2011): Acoustic design shape and topology sensitivity formulations based on adjoint method and bem. *CMES - Computer Modeling in Engineering and Sciences*, vol. 78, no. 2, pp. 77–94.

**McArthur, A. G.** (1966): Weather and grassland fire behaviour. Technical Report Leaflet 100, Commonwealth Department of National Development, Forestry and Timber Bureau, Canberra, ACT, 1966.

**Mell, W.; Jenkins, M. A.; Gould, J.; Cheney, P.** (2007): A physics-based approach to modelling grassland fires. *International Journal of Wildland Fire*, vol. 16, no. 1, pp. 1–22.

**Osher, S.; Sethian, J. a.** (1988): Fronts propagating with curvature-dependent speed: Algorithms based on Hamilton-Jacobi formulations. *Journal of Computational Physics*, vol. 79, no. 1, pp. 12–49.

**Perry, G. L. W.** (1998): Current approaches to modelling the spread of wildland fire: a review. *Progress in Physical Geography*, vol. 22, no. 2, pp. 222–245.

**Peterson, S. H.; Morais, M. E.; Calson, J. M.; Dennison, P. E.; Roberts, D. A.; Moritz, M. A.; Weise, D. R.** (2009): Using HFIRE for spatial modeling of fire in shrublands. Technical Report PSW-RP-259, USDA, Albany, CA, 2009.

**Rehm, R. G.; Mcdermott, R. J.** (2010): Mathematical Modeling of Wildland-Urban Interface Fires. *Monografias de la Real Academia de Ciencias de Zaragoza*, pp. 105–142.

**Richards, G. D.** (1995): A General Mathematical Framework for Modeling Two-Dimensional Wildland Fire Spread. *International Journal Of Wildland Fire*, vol. 5, no. 2, pp. 63–72.

**Rothermel, R. C.** (1972): A mathematical model for predicting fire spread in wildland fuels. Technical Report INT-115, USDA, Ogden, UT, 1972.

**Rothermel, R. C.** (1983): How to predict the spread and intensity of forest and range fires. Technical Report INT-143, USDA, Ogden, UT, 1983.

**Sullivan, A. L.** (2009): Wildland surface fire spread modelling, 1990 - 2007. 1: Physical and quasi-physical models. *International Journal of Wildland Fire*, vol. 18, no. 4, pp. 349–368.

**Sullivan, A. L.** (2009): Wildland surface fire spread modelling, 1990 - 2007. 2: Empirical and quasi-empirical models. *International Journal of Wildland Fire*, vol. 18, no. 4, pp. 369–386.

**Trunfio, G. A.; D'Ambrosio, D.; Rongo, R.; Spataro, W.; Di Gregorio, S.** (2011): A New Algorithm for Simulating Wildfire Spread through Cellular Automata. *ACM Transactions on Modeling and Computer Simulation*, vol. 22, no. 1, pp. 1–26.

**Van Wagner, C. E.** (1998): Modelling Logic and the Canadian Forest Fire Prediction System. *Forestry Chronicle*, vol. 74, no. 1, pp. 50–52.

**Wang, F.; Li, J.; Yang, B.; Hill, N.** (2013): Modeling and simulation of non-newtonian fluid mold filling process with phase change. *CMES - Computer Modeling in Engineering and Sciences*, vol. 95, no. 1, pp. 59–85.

**Yang, B.; Ouyang, J.; Jiang, T.; Liu, C.** (2010): Modeling and simulation of fiber reinforced polymer mold filling process by level set method. *CMES - Computer Modeling in Engineering and Sciences*, vol. 63, no. 3, pp. 191–222.